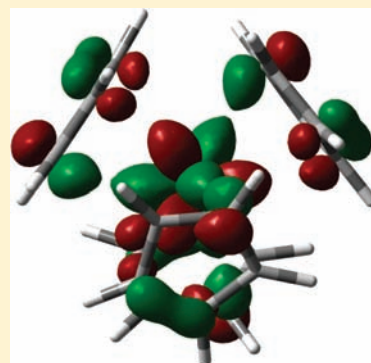


# Does Covalency Increase or Decrease across the Actinide Series? Implications for Minor Actinide Partitioning

Nikolas Kaltsoyannis

Department of Chemistry, University College London, 20 Gordon Street, London WC1H 0AJ, U.K.

**ABSTRACT:** A covalent chemical bond carries the connotation of overlap of atomic orbitals between bonded atoms, leading to a buildup of the electron density in the internuclear region. Stabilization of the valence 5f orbitals as the actinide series is crossed leads, in compounds of the minor actinides americium and curium, to their becoming approximately degenerate with the highest occupied ligand levels and hence to the unusual situation in which the resultant valence molecular orbitals have significant contributions from both actinide and the ligand yet in which there is little atomic orbital overlap. In such cases, the traditional quantum-chemical tools for assessing the covalency, e.g., population analysis and spin densities, predict significant metal–ligand covalency, although whether this orbital mixing is really covalency in the generally accepted chemical view is an interesting question. This review discusses our recent analyses of the bonding in  $\text{AnCp}_3$  and  $\text{AnCp}_4$  ( $\text{An} = \text{Th}–\text{Cm}$ ;  $\text{Cp} = \eta^5\text{-C}_5\text{H}_5$ ) using both the traditional tools and also topological analysis of the electron density via the quantum theory of atoms-in-molecules. I will show that the two approaches yield rather different conclusions and suggest that care must be taken when using quantum chemistry to assess metal–ligand covalency in this part of the periodic table. The implications of this work for minor actinide partitioning from nuclear wastes are discussed; minor actinide extractant ligands based on nitrogen donors have received much attention in recent years, as have comparisons of the extent of covalency in actinide–nitrogen bonding with that in analogous lanthanide systems via quantum-chemical studies employing the traditional tools for assessing the covalency.



## 1. BACKGROUND: SEPARATION OF THE MINOR ACTINIDES FROM POST-PUREX NUCLEAR WASTES

The reprocessing of spent nuclear fuel centers on the PUREX process, which removes the uranium and plutonium for subsequent refabrication into nuclear fuel.<sup>1</sup> The remaining waste is dominated by fission products such as  $^{137}\text{Cs}$ ,  $^{90}\text{Sr}$ , and the lanthanide (Ln) elements, but it also contains the so-called “minor actinides” (MAs) americium and curium (formed by neutron capture by uranium and plutonium in nuclear reactors). The term “minor actinides” is sometimes used to refer to all of the actinide elements found in the nuclear fuel cycle other than uranium and plutonium, but for the purposes of this article, I will take it to mean americium and curium, on which the vast majority of separation studies have focused. Whereas the bulk of the waste consists of isotopes with short half-lives (typically about 30 years), those of the dominant MA isotopes are several hundred years, and some of their decay daughters (e.g.,  $^{239}\text{Pu}$ ) have half-lives that are orders of magnitude longer. Furthermore, while the fission products are predominantly  $\beta$  and/or  $\gamma$  emitters, the MAs and their long-lived daughters are  $\alpha$  emitters and, as such, are much more hazardous.

It is therefore highly desirable to remove the MAs from the post-PUREX nuclear waste. This will greatly reduce the amount of time the bulk of the waste must be stored for, from many thousand years to 200–300 years and, because the concentration of the MA isotopes in nuclear wastes is low, their removal will drastically reduce the volume of waste that

requires very long-term storage. A further benefit of removal of the MAs will be to reduce the heat load on the storage repository; waste can then be more closely packed together, and the overall volume of the repository will be smaller. Finally, because the recoil of heavy  $\alpha$ -emitting nuclei can cause extensive damage to wasteform matrixes, removing the MAs will significantly reduce the hazards associated with storing the bulk of the waste. Once the MAs have been removed, they can be either stored separately or used in fast neutron (e.g., “Generation IV”) reactors (together with recycled uranium and plutonium) both to generate power and to transmute the MAs to less hazardous isotopes.

There is therefore a great deal of current interest in developing technologies to remove the MAs from post-PUREX nuclear wastes. One possibility is to use molten salt (pyrochemical) processing, either high-temperature melts or ionic liquids.<sup>2</sup> A second possible route is to employ liquid extraction using ligands designed to selectively complex the MAs. This second route is the only practicable approach to removing the MAs from the inventories of liquid high-level waste that already exist around the world but is hampered by the relatively high concentration of lanthanide fission products in nuclear wastes. The presence of the lanthanides is highly undesirable because they have high-neutron-capture cross

**Special Issue:** Inorganic Chemistry Related to Nuclear Energy

**Received:** March 22, 2012

**Published:** June 5, 2012

sections and thus prevent transmutation of the MAs in fast neutron reactors. (The lanthanides present in liquid high-level waste do not come solely from nuclear fission. Gadolinium is added to PUREX process solutions precisely because it has a high-neutron-capture cross section and can thus prevent criticality accidents.) Unfortunately, the chemical similarity of the predominant Ln and MA oxidation state (3+) means that many potential extractants fail to adequately separate the MAs from Ln<sup>III</sup>. The design of suitable ligands for MA extraction is therefore a nontrivial problem, and there is much effort currently being devoted to it.<sup>3–20</sup>

The similar behavior of Ln<sup>III</sup> and the trivalent MAs can be traced to the radial extension of the valence f orbitals. In the 4f series, by the time the 3+ oxidation state is achieved, the f electrons are largely corelike and play little role in chemical bonding. By contrast, the 5f orbitals of the early actinide elements have a larger radial extension than their 4f counterparts, and 5f orbital involvement in the bonding in compounds of the first few actinides is not uncommon.<sup>21</sup> Hence, the bonding in compounds of, for example, uranium, is often found to be more covalent than that in analogous compounds of the first few members of the 4f series. The greater metal–ligand covalency in the early actinides should be particularly apparent in complexes featuring ligands with donor atoms that are softer than the oxygen-donor ligands that are traditional in f element chemistry, and it is therefore logical to design extractant ligands for actinide/lanthanide separation that exploit the possibility of a greater covalency in the 5f series. However, a potential problem with this approach is that the actinides become increasingly lanthanide-like in their chemistry as the 5f series is crossed; the 5f orbitals are stabilized and contracted with increasing atomic number, and the variations in the oxidation state observed for the early actinides are replaced by a dominant trivalent chemistry.<sup>22</sup> The extent to which the MAs americium and curium, which lie in the middle of the actinide series, bond more covalently than their lanthanide counterparts (especially europium and gadolinium), is central to the search for post-PUREX MA-extractant ligands.

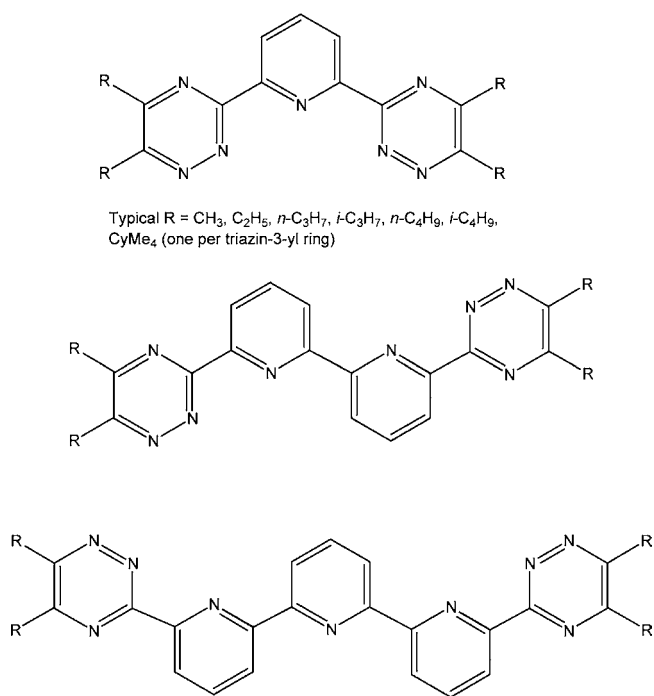
In the United States, much effort continues to be focused on the TALSPEAK (Trivalent Actinide–Lanthanide Separation by Phosphorus reagent Extraction from Aqueous Komplexes) process, in which selective extraction of lanthanides is achieved by contacting a water-soluble aminopolycarboxylate complexant in a concentrated carboxylic acid buffer with a liquid-cation-exchanging extractant in an immiscible organic diluent.<sup>23,24</sup> Sulfur-based ligands have also been shown to selectively bind An<sup>III</sup> over Ln<sup>III</sup>.<sup>25,26</sup> It has been argued, however, that MA separations would ideally follow the “CHON” principle; i.e., the species involved would consist entirely of carbon, hydrogen, oxygen, and nitrogen atoms to render them combustible to safe gaseous products. Because oxygen-based ligands show little selectivity for An<sup>III</sup> over Ln<sup>III</sup>, research (predominantly in Europe) has focused on the design of nitrogen-donor ligands for MA extractants.<sup>3,4,6–8,14,15,17–19</sup> Although such ligands are still classified as hard on the Pearson hard and soft acids and bases scale, it is anticipated that nitrogen is sufficiently softer than oxygen so as to exploit any preference of An<sup>III</sup> for covalent interactions.

The coextraction of the MAs and lanthanides from post-PUREX wastes may be achieved, at least on the laboratory scale, using the DIAMEX process<sup>12</sup> (DIAMide EXtraction; typical extraction ligands include DMDBDTMA, DiMethyl-DiButyl-TetraDecyl-MalonAmide). Subsequently, the SANEX

process (Selective ActiNide EXtraction) separates the MAs from the fission products, and it is here that the nitrogen-donor MA extractants come in. In addition to following the CHON principle, MA extractants must be resistant to radiation damage and also must be able to tolerate low pH because most actinide separation flow sheets operate under highly acidic conditions (neutralization is highly undesirable because it can lead to the formation of unwanted precipitates). DIAMEX has already been demonstrated on a pilot scale and is at about technology readiness level (TRL) 6–7, while SANEX is at about TRL3. [The TRL is a commonly used numerical measure of the maturity of a technology, ranging from 1 (“basic principles observed and reported”) to 9 (“proven through successful operation”); see, for example, [http://esto.nasa.gov/files/TRL\\_definitions.pdf](http://esto.nasa.gov/files/TRL_definitions.pdf).]

A large number of heterocyclic nitrogen-donor potential SANEX extractants have been developed, but most do not survive in low-pH environments. However, one family of ligands that can tolerate high acidity are the 2,6-bis(triazinyl)-pyridines (BTPs; Scheme 1), and because they show separation

**Scheme 1.** BTPs (Upper), 6,6'-Bis(triazinyl)-2,2'-bipyridines (Middle), and Bis(triazinyl)-2,2':6',2"-terpyridines (Lower)



factors for americium or curium versus europium in excess of 100, their chemistry with trivalent f-block cations has been extensively studied by both experimental and computational techniques.<sup>3,4,6,7,14,17,18</sup> Computational study should, in principle, play a particularly valuable role here because the radioactivity of the MAs places severe limits on the experiment, which are feasible at only a few specialist facilities. Much of the computational research has focused on the application of quantum chemistry to assess the extent of covalency in the f element–nitrogen bond and, in particular, to determine if there are differences between the MA and lanthanide compounds that would account for the observed separation factors. These studies have typically employed the traditional tools of quantum chemistry such as charge and population analysis, but it is fair to say that no clear consensus has emerged from

these calculations. For example, Guillaumont used density functional theory (DFT) to study mono-BTP complexes of a range of lanthanides and actinides and concluded that, while there is significant participation of the metal 5f orbitals in the uranium–ligand bond, “there is no significant 5f contribution of americium and curium to the bonding”.<sup>14</sup> By contrast, Petit et al., also on the basis of DFT calculations, stated that “donation on f(Cm) orbitals seems to act as a determining factor in Cm<sup>III</sup> selective complexation to BTP” and that “covalency is ... higher within the Cm–BTP bond [than the Gd equivalent]”.<sup>20</sup> Miguiditchian et al. studied the complexation of trivalent actinides and lanthanides with ADPTZ (another multidentate nitrogen-donor ligand) and also found “a greater degree of covalence in the actinide–nitrogen bonds as compared to lanthanide–nitrogen bonds”, although this was attributed to “charge transfer from the  $\sigma$  orbitals of the ligand to the 6d and 5f orbitals of the actinide cation”.<sup>19</sup>

In light of this, it is perhaps not surprising that, as recently as 2010, Girnt et al. stated “the level of understanding of BTPs’ selectivity on a molecular level is insufficient to target the design of new, more efficient and selective partitioning reagents or fine-tune partitioning process conditions. Such advances are presently empirical, on a trial and error basis”.<sup>13</sup>

The ongoing search for the origin of the ability of BTPs, and successor ligands such as 6,6'-bis(triazinyl)-2,2'-bipyridines and bis(triazinyl)-2,2':6,2''-terpyridines (Scheme 1),<sup>18</sup> to effect the separation of MAs from lanthanides provides the backdrop to this article, the principal focus of which is our recent work probing the covalency in the actinide–carbon bond as the 5f series is crossed. (It should be noted that there are many factors that contribute to the efficacy of MA separation. In addition to the metal–ligand covalency, which is the target of this article, the solubility, complexation kinetics, thermodynamic formation constants, outer-sphere solvent effects, etc., are all known to be important.) These studies were stimulated by our concern that the traditional quantum-chemical measurements of the covalency can lead to counterintuitive results when applied to bonding trends across the actinide elements and led us to explore alternative analysis techniques, in particular the quantum theory of atoms-in-molecules (QTAIM), developed by the late Richard Bader.<sup>27</sup> As we shall see, QTAIM analysis yields conclusions that are rather different from those of, for example, orbital composition and spin-density calculations and that sit rather more comfortably with well-established trends in actinide chemistry.

## 2. DIFFERENT TOOLS YIELD DIFFERENT CONCLUSIONS

In 2007, Prodan et al. published the results of a screened hybrid DFT study of AnO<sub>2</sub> (An = Th–Es).<sup>28</sup> Analysis of the spin densities on the formally An<sup>IV</sup> centers revealed that, although the data for early members of the series are close to the formal expectations, there are increasing deviations from the formal values as the actinide becomes heavier. There are enhancements of the actinide spin densities for americium, and in particular curium, as shown in Figure 1, attributed by Prodan et al. to the actinide borrowing oxygen spin density, with the mechanism for this process being the increasing degeneracy between the actinide 5f orbitals and the oxygen 2p levels across the series. On the basis of these spin-density data, the authors concluded that, contrary to the generally perceived view of actinide chemistry, the covalency actually *increases* toward the center of the 5f series.

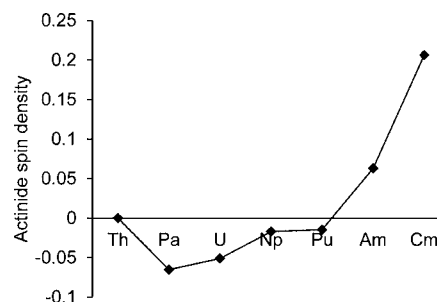


**Figure 1.** Metal spin densities for AnO<sub>2</sub>. Values quoted are the differences from the formal value for An<sup>IV</sup>. Data from ref 28.

We were keen to explore this suggestion in a molecular context and embarked on a study of the electronic structure and bonding in AnCp<sub>4</sub> from thorium to curium (Cp = η<sup>5</sup>-C<sub>5</sub>H<sub>5</sub>).<sup>29</sup> It is well established that the electronic structure of these systems is pseudotetrahedral;<sup>30</sup> in ThCp<sub>4</sub>, the eight highest occupied molecular orbitals (HOMOs) are composed largely of the Cp π<sub>2,3</sub> levels (those that contain a single vertical node perpendicular to the plane of the Cp rings), with an admixture from the metal's d and f orbitals. These eight molecular orbitals (MOs) split into three groups, of pseudo e, t<sub>2</sub>, and t<sub>1</sub> (HOMO) symmetry, strongly reminiscent of a tetroxo or tetrahalide complex.<sup>31–33</sup> As the actinide series is crossed, the additional electrons occupy metal-based orbitals. Figure 2 shows our recent valence MO diagram for UCp<sub>4</sub>,<sup>29</sup> in which the two highest occupied α-spin orbitals house the two 5f electrons expected of a U<sup>IV</sup> center, and Figure 3 presents energy-level diagrams for all AnCp<sub>4</sub> from thorium to curium. The latter figure shows that the energies of the e, t<sub>2</sub>, and t<sub>1</sub> MOs are largely unaltered from thorium to plutonium, in contrast to the 5f-based orbitals, which are very significantly stabilized, as noted previously.<sup>16,34</sup>

Figure 4 shows the actinide contribution to the pseudo e, t<sub>2</sub>, and t<sub>1</sub> Cp π<sub>2,3</sub>-based MOs. The metal 6d contribution to the e levels decreases slightly as the 5f series is crossed. The 6d contribution to the t<sub>2</sub> MOs is approximately half that of the e and initially rises before decreasing again in the latter systems. Most notably, the metal 5f contribution to the Cp-based HOMOs (t<sub>1</sub>) rises steadily from thorium to americium, to >30% in the latter, before decreasing dramatically in CmCp<sub>4</sub>.

The significant increase in the metal 5f contribution to the t<sub>1</sub> orbitals from thorium to americium would appear to support the conclusion of Prodan et al. We subsequently probed AnCp<sub>3</sub> for the same metals,<sup>35</sup> and Mulliken population analysis of the highest Cp π<sub>2,3</sub>-based levels of AnCp<sub>3</sub> finds, as for AnCp<sub>4</sub>, that the metal 5f contribution steadily rises, peaking at americium. For AnCp<sub>3</sub>, we also calculated metal spin densities, and these are shown in Figure 5 for the pure and hybrid versions of the PBE functional.<sup>36–38</sup> The trend in these is similar to that observed in AnO<sub>2</sub>; there is a slight reduction from the formal An<sup>III</sup> value for the early members of the series and then a sharp increase to AmCp<sub>3</sub> before a dramatic reduction to CmCp<sub>3</sub>. Thus, AnCp<sub>3</sub> and AnO<sub>2</sub> behave similarly, with the peak in the spin density coming one element earlier in the trivalent series, tying in with the large americium 5f contribution to the highest Cp π<sub>2,3</sub>-based orbitals.

We had previously observed, in a study of M[N(EPR<sub>2</sub>)<sub>2</sub>]<sub>3</sub> (M = La, Ce, Pr, Pm, Eu, U, Np, Pu, Am, Cm; E = O, S, Se, Te; R = H, <sup>1</sup>Pr, Ph),<sup>16</sup> large 5f contributions to formally ligand-based levels, as well as large 5f atomic populations, in the middle of

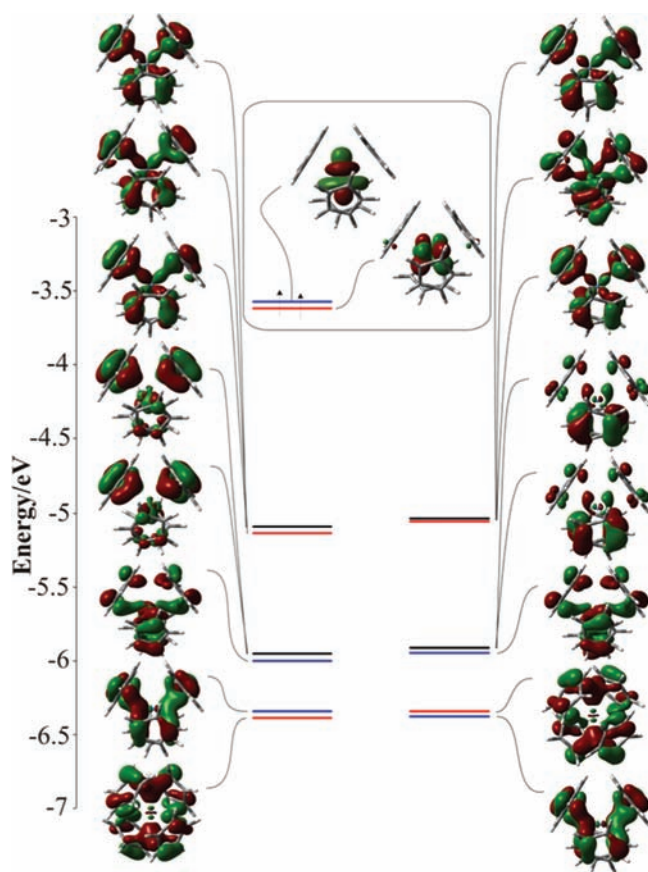


**Figure 2.** Valence MO energy-level diagram for  $\text{UCp}_4$  showing the  $e$  (at most negative energy),  $t_2$ , and  $t_1$  Cp  $\pi_{2,3}$ -based levels and the metals' 5f-based electrons (least negative energy). Red indicates a symmetry MOs (in  $S_4$ ), blue b, and black e.  $\alpha$ -Spin orbitals are shown on the left-hand side and  $\beta$  on the right. From ref 29 (<http://pubs.rsc.org/en/Content/ArticleLanding/2010/DT/c000704h>). Reproduced with permission of The Royal Society of Chemistry.

the actinide series. We suggested that it is the energy match of the 5f and ligand orbitals that generates this effect, and the work of Prodan et al. and our own efforts on  $\text{AnCp}_3$  and  $\text{AnCp}_4$  strongly indicate that this is a common phenomenon; the 5f manifold stabilizes across the series such that it moves through the highest ligand-based orbitals at the MAs.

The question arises as to whether this enhanced orbital mixing should be equated with enhanced covalency. Perturbation theory holds that, to first order, the mixing of MOs  $\phi_i$  and  $\phi_j$  is governed by the mixing coefficient  $t_{ij}^{(1)}$ , where

$$t_{ij}^{(1)} \propto \frac{-S_{ij}}{\epsilon_i - \epsilon_j}$$

Here,  $S_{ij}$  is the overlap between the orbitals and the denominator is the difference in their energies. Thus, large orbital mixings can arise when  $\phi_i$  and  $\phi_j$  are close in energy, without there necessarily being significant orbital overlap. This is exactly the situation we find in the middle of the actinide series, as illustrated in Figure 6, which shows one component of the pseudo  $t_1$  (Cp  $\pi_{2,3}$ -based) orbitals of  $\text{UCp}_4$  and  $\text{AmCp}_4$ .<sup>29</sup> The 5f contribution to the americium orbital is much larger than that in the uranium compound, yet clearly there is more metal–ligand overlap in the latter. Thus, if we accept orbital mixing as the measure of the covalency, then  $\text{AmCp}_4$  is the more covalent compound, yet I believe that most chemists

require a buildup of the electron density in the internuclear region for a bond to be described as covalent; by this measure, the uranium–carbon bond is the more covalent.

It is worth noting that orbital energy levels are by no means well-defined for all quantum-chemical methodologies. In the multiconfigurational approach,<sup>39,40</sup> for example, which we have recently employed to study a variety of f element organometallics, including cyclooctatetraenyl and pentalene species and  $\text{CeCp}_3$ ,<sup>41–44</sup> orbital energy levels lose their meaning. The use of measures of the covalency that depend on orbital energy differences is inappropriate in such circumstances.

In order to probe further the nature of the actinide–Cp bond, we turned to the QTAIM of Bader and co-workers,<sup>27,45</sup> which focuses on the properties of the molecular electron density rather than the orbital structure. This approach has been used extensively by many workers to address the electronic structure and bonding in a wide variety of molecules and solids, including transition-metal organometallics,<sup>46,47</sup> but when we began our study, we were aware of only one previous application of the QTAIM to the actinides.<sup>48</sup> We have found the approach to be a very useful tool, not only in Cp systems, which are the focus of this article, but subsequently for a variety of other f element compounds.<sup>49–52</sup> The QTAIM tells us that there is one bond critical point (BCP) between each pair of atoms that are bonded to one another, with the BCP being the point of lowest electron density along the bond path—the line of maximum electron density between two bonded atoms. Chemical bonding interactions may be characterized and classified according to the properties of the electron and energy densities at these BCPs, and we have focused on the electron density  $\rho$ , its Laplacian  $\nabla^2\rho$ , and the total electronic energy density  $H$  (the sum of the kinetic and potential energy densities). Values of  $\rho$  greater than 0.2 are typical of covalent bonds, and  $\nabla^2\rho$  is generally significantly less than zero for such bonds,<sup>45</sup> reflecting the concentration of the electron density along the bond path linking the bonded atoms.  $H$  at the BCP is negative for interactions with significant sharing of electrons, with its magnitude reflecting the “covalence” of the interaction.<sup>53</sup>

QTAIM analysis of  $\text{AnCp}_4$ <sup>29</sup> and  $\text{AnCp}_3$ <sup>35</sup> reveals very little metal–carbon covalency, as is evidenced by a comparison of the computed BCP data with those from a range of other systems studied either by us or others. For example, the energy density at the uranium–carbon BCPs in  $\text{UCp}_4$  is more than 10 times smaller than that in  $\text{UF}_3\text{CO}$ <sup>48</sup> and more than 30 times smaller than for the metal–carbon bonds in  $\text{M}(\text{CO})_6$  ( $\text{M} = \text{Cr}, \text{Mo}, \text{W}$ ).<sup>29</sup> The electron densities at the actinide–carbon BCPs are shown for  $\text{AnCp}_4$  and  $\text{AnCp}_3$  in Figure 7. All of these values are very small and, as might be expected for  $\text{An}^{\text{III}}$  versus  $\text{An}^{\text{IV}}$ , are slightly larger in the trivalent compounds. Most significantly, following a small increase from thorium to uranium, the BCP electron densities decrease as the series is crossed to the MAs. Thus, as evidenced by the QTAIM data, the metal–carbon bonding in  $\text{AnCp}_4$  and  $\text{AnCp}_3$  is very ionic, increasingly so toward the middle of the actinide series, recovering the traditional view of actinide chemistry.

### 3. ON THE USE OF EARLY ACTINIDES AND LANTHANIDES AS MODELS FOR MA/LANTHANIDE DIFFERENTIATION

The fearsome difficulties associated with experimental MA chemistry has led a number of workers to focus on comparing the structure and bonding in analogous compounds of the early

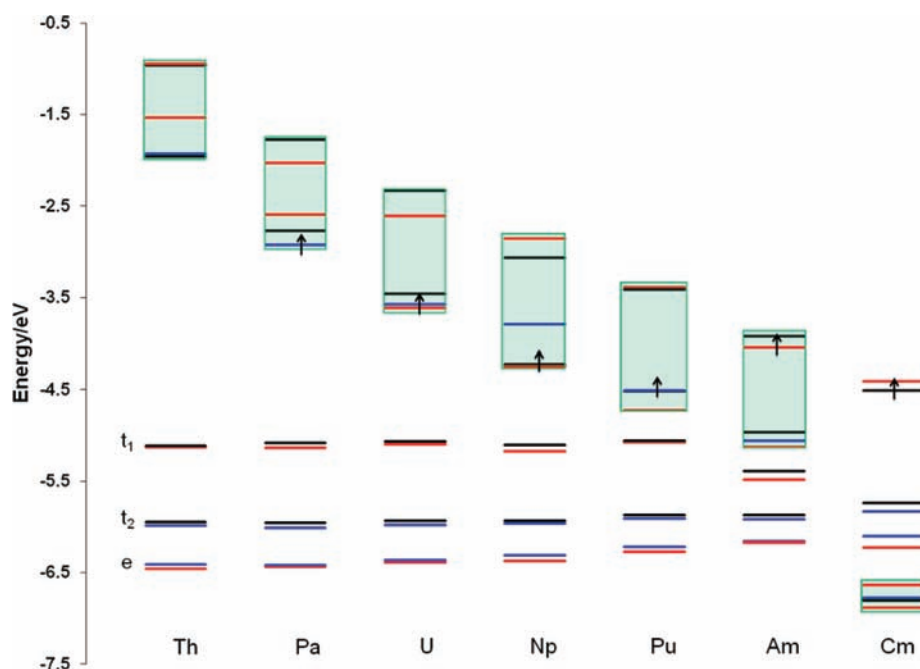


**Figure 3.** MO energy-level diagram for  $\text{AnCp}_4$  showing the e,  $t_2$ , and  $t_1$  Cp  $\pi_{2,3}$ -based levels and the metals' 5f-based orbitals. MOs spanning the a irreducible representation (in the  $S_4$  point group) are given in red, b in blue, and e in black. Green boxes surround the 5f-based orbitals. For the open-shell systems (i.e., all but  $\text{ThCp}_4$ ), the  $\alpha$  levels of a given irreducible representation are shown. The HOMOs are indicated by an arrow (except for  $\text{ThCp}_4$ , where the  $t_1$  Cp  $\pi_{2,3}$ -based combination is the HOMO). From ref 29 (<http://pubs.rsc.org/en/Content/ArticleLanding/2010/DT/c000704h>). Reproduced with permission of The Royal Society of Chemistry.

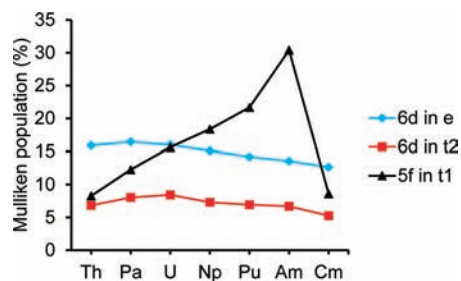


**Figure 4.** Metal contribution (Mulliken populations, %) to the pseudo e,  $t_2$ , and  $t_1$  Cp  $\pi_{2,3}$ -based levels of  $\text{AnCp}_4$ . For open-shell systems, the values quoted are the average of the  $\alpha$ - and  $\beta$ -spin MOs. Data are from ref 29.

4f and 5f elements, in the hope that these systems will serve as mimics for the comparison between the MAs and middle lanthanides such as europium and gadolinium. Much of this work has centered on comparing  $\text{Ln}^{\text{III}}$  with  $\text{An}^{\text{III}}$  in compounds

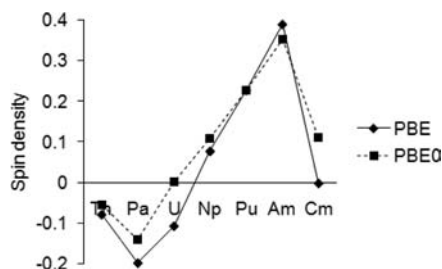


**Figure 5.** Metal spin densities for  $\text{AnCp}_3$ . Values quoted are the differences from the formal value for  $\text{An}^{\text{III}}$ . From ref 35 (<http://pubs.rsc.org/en/Content/ArticleLanding/2011/DT/c0dt01018a>). Reproduced with permission of The Royal Society of Chemistry.

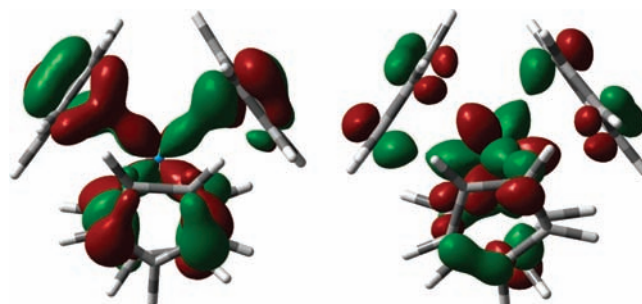


**Figure 6.** Three-dimensional representations of one component of the “ $t_1$ ” MOs of  $\text{UCp}_4$  (left) and  $\text{AmCp}_4$ . The contribution (% Mulliken) of the actinide 5f orbitals to the  $\text{AmCp}_4$  MO is ca. 30%, approximately twice that in  $\text{UCp}_4$ . From ref 29 (<http://pubs.rsc.org/en/Content/ArticleLanding/2010/DT/c000704h>). Reproduced with permission of The Royal Society of Chemistry.

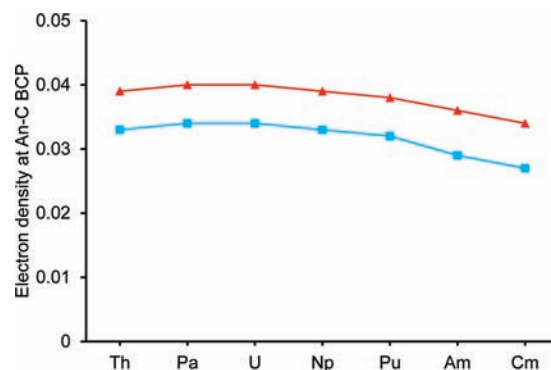


**Figure 7.** Electron density ( $e^-/\text{bohr}^3$ ) at the actinide–carbon BCPs of  $\text{AnCp}_4$  (blue) and  $\text{AnCp}_3$  (red). Data from refs 29 and 35.

of ligands based on donor atoms drawn not only from the first row of the p block but also of their heavier congeners, as noted in section 1. A further refinement has been to choose Ln<sup>III</sup>/An<sup>III</sup> pairs for which the metals' ionic radii are very similar to one another; if significant differences are found in the metal–ligand bond lengths of such pairs, then this is good evidence for differences in bonding.

Gaunt and co-workers have focused on using ligands based on the heavier members of group 16, and the synthesis of trivalent early actinide and lanthanide complexes of imidodiphosphinochalcogenide ligands, featuring sulfur, selenium, and tellurium donors,<sup>9–11</sup> was followed by computational studies from our laboratory.<sup>9,16,54</sup> Experimentally, the uranium–chalcogen bonds were found to be shorter than the corresponding lanthanum–chalcogen, to a significantly larger extent than the difference in the metals' ionic radii, and a similar situation was found for Pu<sup>III</sup> versus Ce<sup>III</sup>. As the group 16 donor atom becomes heavier, these bond-length differences become larger, and our computational studies indicated that this is a result of enhanced covalency, as evidenced by the traditional orbital, charge, and population measures.

In 2009, Arliguie et al. studied the complexation of trivalent cerium, neodymium, and uranium with borohydride ligands.<sup>55</sup> DFT investigation of  $[M(\text{BH}_4)_2(18\text{-crown-6})]^+$  ( $M = \text{Ce}, \text{U}$ ) revealed that the U–BH<sub>4</sub> interaction is more covalent than that in the cerium analogue, as evidenced by Mulliken and natural population analyses. M–BH<sub>4</sub>  $\pi$ -bonding MOs were found to contain significantly more uranium character than cerium, with almost no 4f involvement in the latter set of orbitals. The following year, Meskaldji et al. probed computationally the electronic structure and bonding in dithiolene complexes,  $[M(\text{dddt})_3]^{3-}$  ( $M = \text{Nd}, \text{U}$ ; dddt = 5,6-dihydro-1,4-dithiin-2,3-dithiolate), and noted “striking differences” between the frontier orbitals of the lanthanide and actinide complexes.<sup>56</sup> Specifically, the 5f contribution to the frontier orbitals in the uranium compound was found to be much more significant than the 4f involvement in  $[\text{Nd}(\text{dddt})_3]^{3-}$ , with noticeable metal  $\rightarrow$  ligand back-bonding in  $[\text{U}(\text{dddt})_3]^{3-}$ .

Although the principal focus of the actinide/lanthanide comparisons has been the 3+ oxidation state, we were recently involved in a combined experimental and computational study of analogous cerium(IV) and uranium(IV) compounds,  $M(\text{L})(\text{N}'')_2\text{Cl}$  [ $\text{L} = \text{OCMe}_2\text{CH}_2(\text{CNCH}_2\text{CH}_2\text{NDipp})$ ;  $\text{N}'' = \text{N}(\text{SiMe}_2)_2$ ; ball-and-stick representation of the experimentally determined structure of the uranium molecule shown in Figure 8].<sup>49</sup> X-ray crystallography indicates that the U–C<sub>carbene</sub> distance is not significantly (i.e., within the  $3\sigma$  criterion) different from the Ce–C<sub>carbene</sub> distance, despite the ionic radius of U<sup>IV</sup> being 0.02 Å larger than that of Ce<sup>IV</sup>, while our calculations on model systems found  $r(\text{U}-\text{C}_{\text{carbene}})$  to be ca. 0.06 Å shorter. The Mayer bond order of the Ce–C<sub>carbene</sub> bond was found to be smaller than that for U–C<sub>carbene</sub>, and the metal–carbon BCP data all pointed to a more ionic interaction in the 4f compound. Two years previously, Szigethy et al. explored the Ce<sup>IV</sup>/Pu<sup>IV</sup> comparison and found surprising coordination geometry differences in their 5-bromo-3-hydroxy-2-methylpyran-4-one complexes.<sup>57</sup> The authors speculated that “the larger role of both f and d orbital bonding in Pu(IV) compared to Ce(IV) explains this difference”.

A pattern has clearly emerged from the comparative studies discussed above, and I am happy to conclude that there is greater covalency in the early actinide–ligand bond than in lanthanide equivalents, not only in the sense of orbital mixing

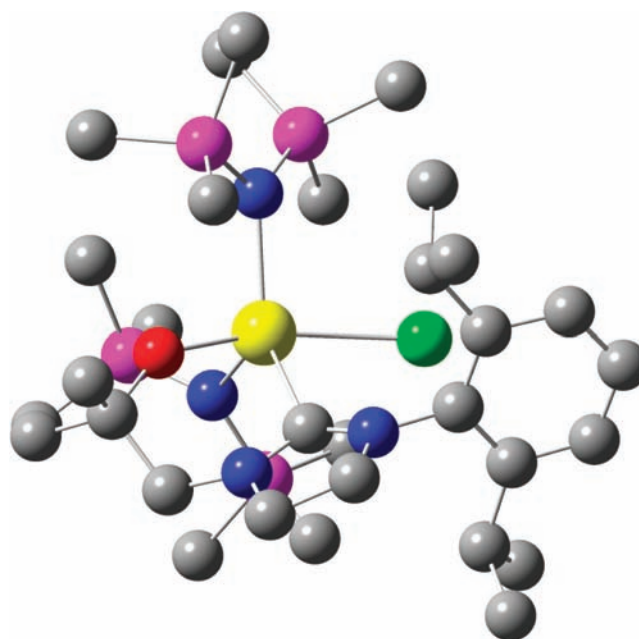


**Figure 8.** Ball-and-stick representation of  $\text{U}(\text{L})(\text{N}'')_2\text{Cl}$  [ $\text{L} = \text{OCMe}_2\text{CH}_2(\text{CNCH}_2\text{CH}_2\text{NDipp})$ ;  $\text{N}'' = \text{N}(\text{SiMe}_2)_2$ ]. Hydrogen atoms omitted for clarity. Color code: U, yellow; Si, magenta; Cl, green; N, blue; O, red; C, gray.

but also orbital overlap and internuclear charge buildup. The traditional analysis tools used in early lanthanide/actinide comparisons yield a consistent and realistic picture of the metal–ligand bonding. However, I am much less convinced that the conclusions drawn from the early f elements are transferable to the chemistry of the MAs and their lanthanide equivalents. It may well be that there is appreciable 5f contribution to valence MOs in compounds of the MAs, but this should not be taken as meaning that the metal–ligand bond is covalent in anything other than an orbital mixing sense. Indeed, in our study of imidodiphosphinochalcogenide complexes of the actinides from uranium through to curium, we noted “It is rather difficult ... to see how differences in f-based covalency between the middle of the lanthanide and actinide series can account for the soft-donor selectivity for the MAs over Eu; the f orbitals are too contracted to engage in covalent bonding.”<sup>16</sup> Our recent QTAIM work on  $\text{AnCp}_3$  and  $\text{AnCp}_4$  lends further weight to this conclusion, and it is noticeable that EXAFS data on curium(III) and europium(III) complexed with *n*-C<sub>3</sub>H<sub>7</sub>–BTP indicate identical solution coordination structures,<sup>6</sup> a conclusion supported computationally, by contrast to the significantly shorter U<sup>III</sup>–BTP versus Ce<sup>III</sup>–BTP bonds.<sup>17</sup>

#### 4. CONCLUDING REMARKS

Our studies of  $\text{AnCp}_4$  and  $\text{AnCp}_3$  indicate that the metal–carbon bond becomes both more covalent (on the basis of orbital mixing and spin densities) and more ionic (as evidenced by the QTAIM data) as the actinide series is crossed, precluding a simple answer to the title question. We must, therefore, be very clear as to what we mean when discussing covalency in the 5f series, especially when using this concept as a basis for interpreting experimental data such as the enhanced MA separation factors achieved by BTP and related ligands. I am not aware of other areas of the periodic table where significant valence orbital mixing does not lead to internuclear

charge buildup; once again, the unique challenge presented by the f elements comes to the fore.

## AUTHOR INFORMATION

### Notes

The authors declare no competing financial interest.

## ACKNOWLEDGMENTS

I am grateful to Dr. Andrew Kerridge and Abigail Mountain for reading and commenting on drafts of this manuscript and to the reviewers for their helpful comments.

## REFERENCES

- (1) *The Nuclear Fuel Cycle: From Ore to Waste*; Wilson, P. D., Ed.; Oxford University Press: Oxford, U.K., 1996.
- (2) Madic, C. *Actinide and Fission Product Partitioning and Transmutation*; OECD/NEA: Madrid, 2000.
- (3) Benay, G.; Schurhammer, R.; Desaphy, J.; Wipff, G. *New J. Chem.* **2011**, *35*, 184.
- (4) Benay, G.; Schurhammer, R.; Wipff, G. *Phys. Chem. Chem. Phys.* **2010**, *12*, 11089.
- (5) Bhattacharyya, A.; Ghanty, T. P.; Mohapatra, P. K.; Manchanda, V. J. *Inorg. Chem.* **2011**, *50*, 3913.
- (6) Denecke, M. A.; Rossberg, A.; Panak, P. J.; Weigl, M.; Schimmelpfennig, B.; Geist, A. *Inorg. Chem.* **2005**, *44*, 8418.
- (7) Drew, M. G. B.; Guillauneux, D.; Hudson, M. J.; Iveson, P. B.; Russell, M. L.; Madic, C. *Inorg. Chem. Commun.* **2001**, *4*, 12.
- (8) Foreman, M. R. S. J.; Hudson, M. J.; Drew, M. G. B.; Hill, C.; Madic, C. *Dalton Trans.* **2006**, 1645.
- (9) Gaunt, A. J.; Reilly, S. D.; Enriquez, A. E.; Scott, B. L.; Ibers, J. A.; Sekar, P.; Ingram, K. I. M.; Kaltsoyannis, N.; Neu, M. P. *Inorg. Chem.* **2008**, *47*, 29.
- (10) Gaunt, A. J.; Scott, B. L.; Neu, M. P. *Chem. Commun.* **2005**, 3215.
- (11) Gaunt, A. J.; Scott, B. L.; Neu, M. P. *Angew. Chem., Int. Ed.* **2006**, *45*, 1638.
- (12) Geist, A.; Hill, C.; Modolo, G.; Foreman, M. R. S. J.; Weigl, M.; Gompper, K.; Hudson, M. J. *Solvent Extr. Ion Exch.* **2006**, *24*, 463.
- (13) Girnt, D.; Roesky, P. W.; Geist, A.; Ruff, C. M.; Panak, P. J.; Denecke, M. A. *Inorg. Chem.* **2010**, *49*, 9627.
- (14) Guillaumont, D. *J. Phys. Chem. A* **2004**, *108*, 6893.
- (15) Hill, C.; Guillauneux, D.; Berthon, L.; Madic, C. *J. Nucl. Sci. Technol.* **2002**, *Sup. 3*, 309.
- (16) Ingram, K. I. M.; Tassell, M. J.; Gaunt, A. J.; Kaltsoyannis, N. *Inorg. Chem.* **2008**, *47*, 7824.
- (17) Iveson, P. B.; Rivière, C.; Guillauneux, D.; Nierlich, M.; Thuéry, P.; Ephritikhine, M.; Madic, C. *Chem. Commun.* **2001**, 1512.
- (18) Lewis, F. W.; Harwood, L. M.; Hudson, M. J.; Drew, M. G. B.; Modolo, G.; Syupla, M.; Desreux, J. F.; Bouslimani, N.; Vidick, G. *Dalton Trans.* **2010**, *39*, 5172.
- (19) Miguiditchian, M.; Guillauneux, D.; Guillaumont, D.; Moisy, P.; Madic, C.; Jensen, M. P.; Nash, K. L. *Inorg. Chem.* **2005**, *44*, 1404.
- (20) Petit, L.; Adamo, C.; Maldivi, P. *Inorg. Chem.* **2006**, *45*, 8517.
- (21) Kaltsoyannis, N.; Hay, P. J.; Li, J.; Blaudeau, J.-P.; Bursten, B. E. In *The Chemistry of the Actinide and Transactinide Elements*, 3rd ed.; Morss, L. R., Edelstein, N., Fuger, J., Eds.; Springer: Berlin, 2006; p 1893.
- (22) Kaltsoyannis, N.; Scott, P. *The f elements*; Oxford University Press: Oxford, U.K., 1999.
- (23) Braley, J. C.; Grimes, T. S.; Nash, K. L. *Ind. Eng. Chem. Res.* **2012**, *51*, 629.
- (24) Nilsson, M.; Nash, K. L. *Solvent Extr. Ion Exch.* **2007**, *25*, 665.
- (25) Jensen, M. P.; Bond, A. H. *Radiochim. Acta* **2002**, *90*, 205.
- (26) Jensen, M. P.; Bond, A. H. *J. Am. Chem. Soc.* **2002**, *124*, 9870.
- (27) Bader, R. F. W. *Atoms in Molecules: A Quantum Theory*; OUP: Oxford, U.K., 1990.
- (28) Prodan, I. D.; Scuseria, G. E.; Martin, R. L. *Phys. Rev. B* **2007**, *76*, 033101.
- (29) Tassell, M. J.; Kaltsoyannis, N. *Dalton Trans.* **2010**, *39*, 6719.
- (30) Bursten, B. E.; Casarin, M.; DiBella, S.; Fang, A.; Fragalà, I. L. *Inorg. Chem.* **1985**, *24*, 2169.
- (31) Bursten, B. E.; Green, J. C.; Kaltsoyannis, N. *Inorg. Chem.* **1994**, *33*, 2315.
- (32) Green, J. C.; Guest, M. F.; Hillier, I. H.; Jarrett-Sprague, S. A.; Kaltsoyannis, N.; MacDonald, M. A.; Sze, K. H. *Inorg. Chem.* **1992**, *31*, 1588.
- (33) Kaltsoyannis, N. *Chem. Phys. Lett.* **1997**, *274*, 405.
- (34) Bursten, B. E.; Rhodes, L. F.; Strittmatter, R. J. *J. Am. Chem. Soc.* **1989**, *111*, 2756.
- (35) Kirker, I.; Kaltsoyannis, N. *Dalton Trans.* **2011**, *40*, 124.
- (36) Adamo, C.; Barone, V. *J. Chem. Phys.* **1999**, *110*, 6158.
- (37) Perdew, J. P.; Burke, K.; Ernzerhof, M. *Phys. Rev. Lett.* **1996**, *77*, 3865.
- (38) Perdew, J. P.; Burke, K.; Ernzerhof, M. *Phys. Rev. Lett.* **1997**, *78*, 1396.
- (39) Roos, B. O.; Taylor, P. R. *Chem. Phys.* **1980**, *48*, 157.
- (40) Malmqvist, P. A.; Roos, B. O.; Schimmelpfennig, B. *Chem. Phys. Lett.* **2002**, *357*, 230.
- (41) Kerridge, A.; Coates, R.; Kaltsoyannis, N. *J. Chem. Phys.* **2009**, *113*, 2896.
- (42) Kerridge, A.; Kaltsoyannis, N. *J. Phys. Chem. A* **2009**, *113*, 8737.
- (43) Coates, R.; Coreno, M.; DeSimone, M.; Green, J. C.; Kaltsoyannis, N.; Kerridge, A.; Narband, N.; Sella, A. *Dalton Trans.* **2009**, 5943.
- (44) Kerridge, A.; Kaltsoyannis, N. *C. R. Chimie* **2010**, *13*, 853.
- (45) Matta, C. F.; Boyd, R. J. In *The quantum theory of atoms in molecules*; Matta, C. F., Boyd, R. J., Eds.; Wiley-VCH: Weinheim, Germany, 2007; p 1.
- (46) Farrugia, L. J.; Evans, C.; Lentz, D.; Roemer, M. *J. Am. Chem. Soc.* **2009**, *131*, 1251.
- (47) Gatti, C.; Lasi, D. *Faraday Discuss.* **2007**, *135*, 55.
- (48) Petit, L.; Joubert, L.; Maldivi, P.; Adamo, C. *J. Am. Chem. Soc.* **2006**, *128*, 2190.
- (49) Arnold, P. L.; Turner, Z. R.; Kaltsoyannis, N.; Pelekanaki, P.; Bellabarba, R. M.; Tooze, R. P. *Chem.—Eur. J* **2010**, *16*, 9623.
- (50) Saleh, L. M. A.; Hassomal Birjukumar, K.; Protchenko, A. V.; Schwarz, A. D.; Aldridge, S.; Jones, C.; Kaltsoyannis, N.; Mountford, P. *J. Am. Chem. Soc.* **2011**, *133*, 3836.
- (51) Mansell, S. M.; Kaltsoyannis, N.; Arnold, P. L. *J. Am. Chem. Soc.* **2011**, *133*, 9036.
- (52) Blake, M. P.; Kaltsoyannis, N.; Mountford, P. *J. Am. Chem. Soc.* **2011**, *133*, 15358.
- (53) Cremer, D.; Kraka, E. *Angew. Chem., Int. Ed.* **1984**, *23*, 627.
- (54) Ingram, K. I. M.; Kaltsoyannis, N.; Gaunt, A. J.; Neu, M. P. *J. Alloys Compd.* **2007**, *444–445*, 369.
- (55) Arliguie, T.; Belkhari, L.; Bouaoud, S.-E.; Thuéry, P.; Villiers, C.; Boucekkine, A.; Ephritikhine, M. *Inorg. Chem.* **2009**, *48*, 221.
- (56) Meskaldji, S.; Belkhari, L.; Arliguie, T.; Fourmigue, M.; Ephritikhine, M.; Boucekkine, A. *Inorg. Chem.* **2010**, *49*, 3192.
- (57) Szigethy, G.; Xu, J.; Teat, S. J.; Shuh, D. K.; Raymond, K. N. *Eur. J. Inorg. Chem.* **2008**, *13*, 2143.